Human scotopic dark adaptation: Comparison of recoveries of psychophysical threshold and ERG *b*-wave sensitivity

Rasa Ruseckaite — ISCRR, Monash University, Melbourne, Vic, Australia, & ARC Centre of Excellence in Vision Science, Australian National University, Canberra, ACT, Australia

Trevor D. Lamb — John Curtin School of Medical Research and ARC Centre of Excellence in Vision Science, Australian National University, Canberra, ACT, Australia

Michael J. Pianta — Department of Optometry and Vision Sciences, University of Melbourne, Melbourne, Vic, Australia

Allison M. Cameron — John Curtin School of Medical Research and ARC Centre of Excellence in Vision Science, Australian National University, Canberra, ACT, Australia

We have compared the time course of dark adaptation of the human scotopic visual system, measured psychophysically and from the *b*-wave of the electroretinogram (ERG), for bleaches ranging from a few percent to near total. We also measured light adaptation, in order to apply a "Crawford transformation" to convert the raw measurements of dark adaptation into equivalent background intensities. For both the "psychophysical threshold equivalent" intensity and the "ERG *b*-wave sensitivity equivalent" intensity, the equivalent background declined over much of its range with an "S2" component, though with somewhat different slopes of −0.36 (psychophysical) and −0.22 (ERG) $\log_{10}$ unit min^{-1}, respectively. In addition, the magnitude of the equivalent background was approximately 1 $\log_{10}$ unit lower in the psychophysical experiments than in the ERG experiments. Despite these differences, the two approaches extract a common time course for the decline in level of free opsin following moderately large bleaches. We conclude that the recovery of psychophysical scotopic visual threshold over the S2 region reflects events that are present by the stage of the first synapse of rod vision, stemming ultimately from the presence of unregenerated opsin in the rod outer segments.

Keywords: dark adaptation, psychophysics, rod bipolar cells, equivalent background, electroretinogram, *b*-wave

Citation: Ruseckaite, R., Lamb, T. D., Pianta, M. J., & Cameron, A. M. (2011). Human scotopic dark adaptation: Comparison of recoveries of psychophysical threshold and ERG *b*-wave sensitivity. *Journal of Vision, 11*(8):2, 1–16, http://www.journalofvision.org/content/11/8/2, doi:10.1167/11.8.2.

Introduction

Night vision (scotopic vision) is extraordinarily sensitive, and the human eye is able to detect flashes of large area that are so dim that they produce only a single photoisomerization for every 10,000 rods (Hecht, Shlaer, & Pirenne, 1942; Sakitt, 1972; reviewed in Rodieck, 1998). When the background intensity changes (either increasing or decreasing), the subject's sensitivity usually changes rapidly, provided that the change in intensity is not too large. However, following exposure to extremely bright illumination that "bleaches" an appreciable fraction of the rhodopsin, the recovery of sensitivity upon returning to darkness occurs very slowly. This slow recovery of sensitivity is known as "dark adaptation" or "bleaching adaptation," and psychophysical studies have shown that following a total bleach of the rhodopsin, the observer's visual system can take as long as 50 min to recover (reviewed in Lamb, 1990; Lamb & Pugh, 2004; Rushton, 1965).

The adapting effects that occur following a bleaching exposure consist of reduced sensitivity (elevated threshold for light detection) together with improved spatial and temporal resolution. With increasing post-bleach time, visual sensitivity steadily improves while spatial and temporal integration both increase. It has long been held that these effects are produced by a phenomenon within the visual system equivalent to a "veiling light," at an intensity called the "equivalent background intensity" (Stiles & Crawford, 1932). During post-bleach recovery, the intensity of this veiling light slowly declines (Barlow,

doi: 10.1167/11.8.2 Received March 21, 2011; published July 6, 2011 ISSN 1534-7362

1972; Blakemore & Rushton, 1965; Crawford, 1947; Lamb, 1981).

In an analysis of Pugh's (1975) psychophysical results for the post-bleach recovery of visual threshold, Lamb (1981) reported that for every bleach level, it was possible to distinguish a region over which the recovery of log scotopic threshold declined as a straight line and, furthermore, that the slope of this linear decline was the same, irrespective of the initial bleach. Recovery of this kind was termed the "S2" component of dark adaptation, and its slope in semi-logarithmic coordinates was -0.24 $\log_{10}$ unit min^{-1}. To interpret this behavior, Lamb (1981) suggested that the equivalent background was caused by some photoproduct of bleaching and that the S2 region of recovery represented the exponentially declining level of that photoproduct with time, thereby causing the equivalent background intensity to decline exponentially and the $\log_{10}$ visual threshold to decline with a constant slope.

Experiments with isolated photoreceptors have confirmed that the equivalent background is caused by a bleaching photoproduct within rods, with responses obtained following small bleaching exposures resembling those found in the presence of real background illumination (Cornwall & Fain, 1994; Leibrock & Lamb, 1997; Leibrock, Reuter, & Lamb, 1994). The identity of the bleaching photoproduct underlying the S2 component has been reported to be opsin (Lamb & Pugh, 2004; Lamb, Pugh, Cideciyan, & Jacobson, 1997), which is able to weakly activate the phototransduction cascade and weakly imitate the activated rhodopsin (Rh*) produced by real background light (Cornwall & Fain, 1994; Melia, Cowan, Angleson, & Wensel, 1997).

In recent experiments, we recorded the *b*-wave of the scotopic electroretinogram to examine the dark adaptation recovery of retinal rod bipolar cells (Cameron, Mahroo, & Lamb, 2006; Cameron, Miao, Ruseckaite, Pianta, & Lamb, 2008). In that work, we showed that the post-bleach recovery of *b*-wave flash sensitivity can be described in terms of an equivalent background that fades with an S2 component, and we proposed that (as in psychophysical experiments) the S2 component was caused by the disappearance of opsin (bleached rhodopsin) within the rods, by reconversion to rhodopsin. The aim of the present study is to compare the properties of dark adaptation, as measured psychophysically for the overall visual system and for the *b*-wave of the ERG, in experiments on the same subjects.

Methods

Subjects

The subjects were the four authors, aged from 32 to 59 years; all had normal vision, apart from minor errors of refraction. Ethical approval for the study was obtained from the Australian National University's Human Research Ethics Committee. Prior to participating in the study, subjects provided informed written consent.

Illumination

Two ganzfeld rigs were used. The very dim test stimuli and adapting backgrounds were delivered using a ColorDome desktop ganzfeld stimulator (Diagnosys LLC, MA, USA), driven by a custom Matlab-based program "MatColorDome" written by Mr. Liang Miao. A second ganzfeld, which has been described previously (Cameron et al., 2006), was used for delivery of the intense bleaching illumination and for measurement of pupil size, as well as for the ERG experiments.

Light intensities were measured with a calibrated photometer (IL-1700, fitted with a radiometric barrel and scotopic (Z-CIE) filter; International Light, Newburyport, MA, USA); with the amplified detector SHD033, it was possible to obtain reliable readings down to $\sim 10^{-4}$ cd m^{-2}. Using these measurements, we made slight corrections to the calibration file provided with the ColorDome. Intensities in cd m^{-2} were converted to trolands (Td) by multiplying by the pupil area in mm^2. All intensities are given in scotopic units.

Test and adapting stimuli

In previous dark adaptation studies, psychophysical experiments have typically used light stimuli in the form of small diameter patches presented in the parafovea, whereas ERG experiments have employed full-field illumination; in this study, we have used both. Circular patches of illumination were obtained by placing a piece of black card with an appropriate aperture in front of the ColorDome; the apertures used subtended diameters of 5°, 10°, 15°, and 20° of visual angle when viewed from a distance of 28 cm, corresponding to areas of 20, 80, 180, and 315 deg^2. With this aperture arrangement, the adapting field (if used) was spatially coincident with the test flash. The subject centered the patch at 12° in the nasal field by fixating a red LED through a second aperture in the card that was covered with red acetate filter; this filter prevented passage of blue light but enabled the fixation LED to be seen. Under full-field viewing conditions, the subject observed the test flashes and backgrounds within the interior of the ColorDome stimulator, at the normal viewing distance, while fixating a central red LED.

All test and adapting stimuli were blue ($\lambda_{max} = 455$ nm). Test flashes were brief (2–200 ms) and were delivered at an inter-flash interval of 3 s. The dark-adapted threshold with full-field 200-ms stimuli was lower than the ColorDome could reliably deliver, and so some experiments

were performed with a 1.2 log unit neutral density filter. The reported intensities have been adjusted accordingly.

Bleach delivery

Bleaches were delivered with up to 12 ultrabright white LEDs, long pass filtered at 520 nm (HT101, Lee Filters) to remove blue light, so as to minimize any possible damage from high-intensity short-wavelength illumination; using LEDs, there was no need to filter out infrared. The maximum luminous intensity that could be delivered was ~10,000 cd m^{-2}. The duration of the bleaches ranged from 6 to 30 s (except in one ERG experiment where a 60-s exposure was used), and during each bleach, an image of the test eye was recorded on videotape. The magnitude of the bleach was estimated by numerically solving Equation A12 of Mahroo and Lamb (2004), using the parameter values $\nu = 0.084$ min^{-1} for the limiting rate, $K_m = 0.18$ for the semi-saturation constant, and Q_e (=1/σ) = $10^{6.7}$ Td s for the bleaching constant. The subjects often found it difficult to keep their eyelids fully open during the larger bleaches with prolonged exposures; although we attempted to account for eyelid drooping using video images, it is possible that our estimates of bleach delivery for the largest bleaches may be inaccurate.

The bulk of the ERG experiments had been performed previously, using a set of nominal bleaching levels; for the psychophysical experiments, we chose a different set of nominal bleach levels that covered the range more uniformly. The bleach intensity-time products (in Td s) and the calculated bleach levels (%) are given in the relevant part of the Results section, in Tables 2 and 3.

Procedure for psychophysical experiments

Psychophysical experiments and ERG experiments were performed on one eye (nominated by the subject). After a period in dim lighting, two drops of 1% tropicamide were instilled to fully dilate the pupil (diameter ~7 mm), and the subject was then dark-adapted for a further 15–20 min before testing; if necessary, another drop was applied 90 min later. The fellow eye was covered with a black patch. Two subjects wore spectacles to enable them to accommodate on the fixation spot.

Following the initial period of dark adaptation, the subject's fully dark-adapted threshold was measured for a period of at least 5 min. Thereafter, either a light adaptation or a dark adaptation experiment was performed. For light adaptation experiments, each background was switched on for 30 s, and then threshold measurements were made for at least 5 min; background intensities ranged from 10^{-6} to 100 scotopic cd m^{-2}.

For dark adaptation experiments, the subject moved to the main ganzfeld sphere to receive the bleach, and then quickly returned to the ColorDome for post-bleach measurement of threshold for a period of up to 45 min.

Estimation of threshold

Visual thresholds were estimated using a staircase procedure, modified from Cideciyan, Pugh, Lamb, Huang, and Jacobson (1997). Each test flash presentation was cued by an audio tone. The subject used a push-button gamepad (Logitech) to indicate whether or not the test flash had been seen. If the test flash was reported as "not seen," the flash strength was increased by 0.1 log unit. If it was reported as "seen," the flash strength was reduced; the magnitude of this reduction had a mean value of 0.3 log unit but with a Gaussian-distributed random component that was typically set to have a standard deviation of 0.1 log unit. This random component was introduced in

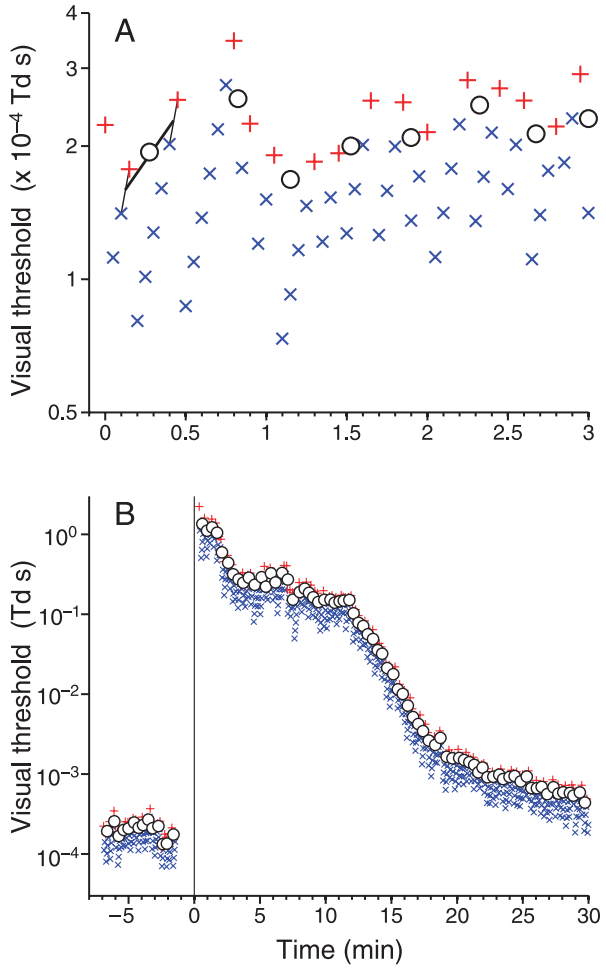

Figure 1. Demonstration of the staircase method for estimating visual threshold (A) in the steady dark-adapted state and (B) prior to and following a large bleach (~85%). The "×" and "+" symbols plot the flash strength delivered, with × denoting "not seen" (next intensity increases by 0.1 log unit) and + denoting "seen" (next intensity decreases on average by 0.3 log unit). The circles (○) plot our estimates of threshold, averaged from pairs of successive reversals from "not seen" to "seen." In (A), the initial two reversals are joined by thin steep lines, and the thick line joins the mean flash times and strengths.

order to reduce the subject's expectation of when the stimulus would next be visible and also to avoid the use of identically the same set of intensities throughout. The subject was expected to make a response within 3 s of flash presentation and could correct an erroneous button press within that time; however, if no response was made, the test flash strength was not changed, thereby allowing the subject to take a rest without compromising the experiment. The threshold was taken to be the average of the flash strengths for two successive reversals from "not seen" to "seen" (see Figure 1), exactly as in Cideciyan et al. (1997). Alternative approaches might involve taking every reversal, or taking a running average of reversals, but we chose to conform to the previously published approach. By averaging the "not seen" and "seen" intensities, it was effectively assumed that the threshold was midway between these levels; although it is possible that this estimate might be slightly vertically shifted from the true threshold, this will not affect our results as the same procedure was used for light adaptation and dark adaptation.

ERG *b*-wave measurements

The ERG *b*-wave measurements were made on the same four subjects, as described in detail in two recent studies (Cameron et al., 2006, 2008). The results presented in one panel (Figure 7, bottom right) have been replotted from that work, but all other data are new.

Results

Our goals in this study were, first, to determine the time course of dark adaptation and the fading of "equivalent background illumination" in the human rod visual system, as measured both psychophysically and with ERG *b*-wave recordings and, second, to compare the results obtained using the two approaches. This has been achieved by making measurements of psychophysical dark adaptation for four subjects whose ERG *b*-wave recoveries have recently been examined (Cameron et al., 2006, 2008).

In the literature, most measurements of human psychophysical scotopic dark adaptation have been made using test stimuli of relatively small area, presented in the parafovea or mid-periphery and with a flash duration typically of 200 ms (e.g., Cideciyan et al., 2000, 1997; Jackson, Owsley, & McGwin, 1999; Jacobson, Cideciyan, Kemp, Sheffield, & Stone, 1996; Jacobson et al., 1995, 1986; Nordby, Stabell, & Stabell, 1984; Owsley, Jackson, White, Feist, & Edwards, 2001; Pugh, 1975; Sharpe & Nordby, 1990). In contrast, ERG measurements of human scotopic dark adaptation have been made using full-field test stimuli, with very short duration flashes (e.g., Cameron et al., 2006, 2008; Thomas & Lamb, 1999).

For electroretinography, full-field stimulation is required in order to obtain responses of sufficiently large amplitude to keep the signal-to-noise ratio reasonable and to ensure that all rods across the retina are receiving the same intensity of illumination.

For psychophysics, full-field stimulation has been used only rarely (see Frishman, Reddy, & Robson, 1996, for light adaptation, and Roman et al., 2005, for fully dark-adapted thresholds) and has not, to our knowledge, been applied to examine dark adaptation. In order to bridge the gap between the stimuli conventionally used for psychophysical and ERG measurements of human scotopic dark adaptation, we employed a range of stimulus geometries and durations in our psychophysical experiments, and we sought to determine whether these led to any significant differences in recovery. We used circular patches with diameters subtending 5°, 10°, 15°, and 20°, centered 12° in the nasal field, as well as full-field (ganzfeld) stimulation, and we used flash durations ranging from 2 to 200 ms.

Effect of stimulus size and duration on dark-adapted threshold

In Figure 2, we investigate the influence of the duration and size of the test stimulus on the measured level of fully dark-adapted threshold, for two subjects (R.R., left and T.D.L., right). The upper panels (Figures 2A and 2B) plot the dark-adapted visual threshold in Td s as a function of stimulus duration, for five stimulus sizes, while the lower panels (Figures 2C and 2D) plot the same measurements as a function of stimulus size (area and diameter) for seven stimulus durations. Full-field measurements in Figures 2C and 2D have been plotted at a nominal stimulus area of 13,000 deg^2 (or diameter of 130°, based on the spatial extent of the retina rather than on the size of the visual field); however, the value assumed is not critical. The measurements in Figure 2 are closely consistent with classical results, as reported, for example, by Barlow (1958).

Figures 2A and 2B show that complete temporal summation occurs (Bunsen–Roscoe/Bloch's law) for stimulus durations shorter than about 50 ms, because the threshold quantity of light (in Td s) is constant. On the other hand, for very long stimulus durations, Barlow (1958) showed that the threshold intensity approached a constant, so that the threshold quantity should increase in proportion to stimulus duration, as indicated by the form of the curve at longer durations in Figures 2A and 2B.

Figures 2C and 2D show that partial spatial summation occurs over the investigated range of stimulus sizes. Barlow (1958) showed that complete spatial summation (Ricco's law) occurs only for stimulus areas less than

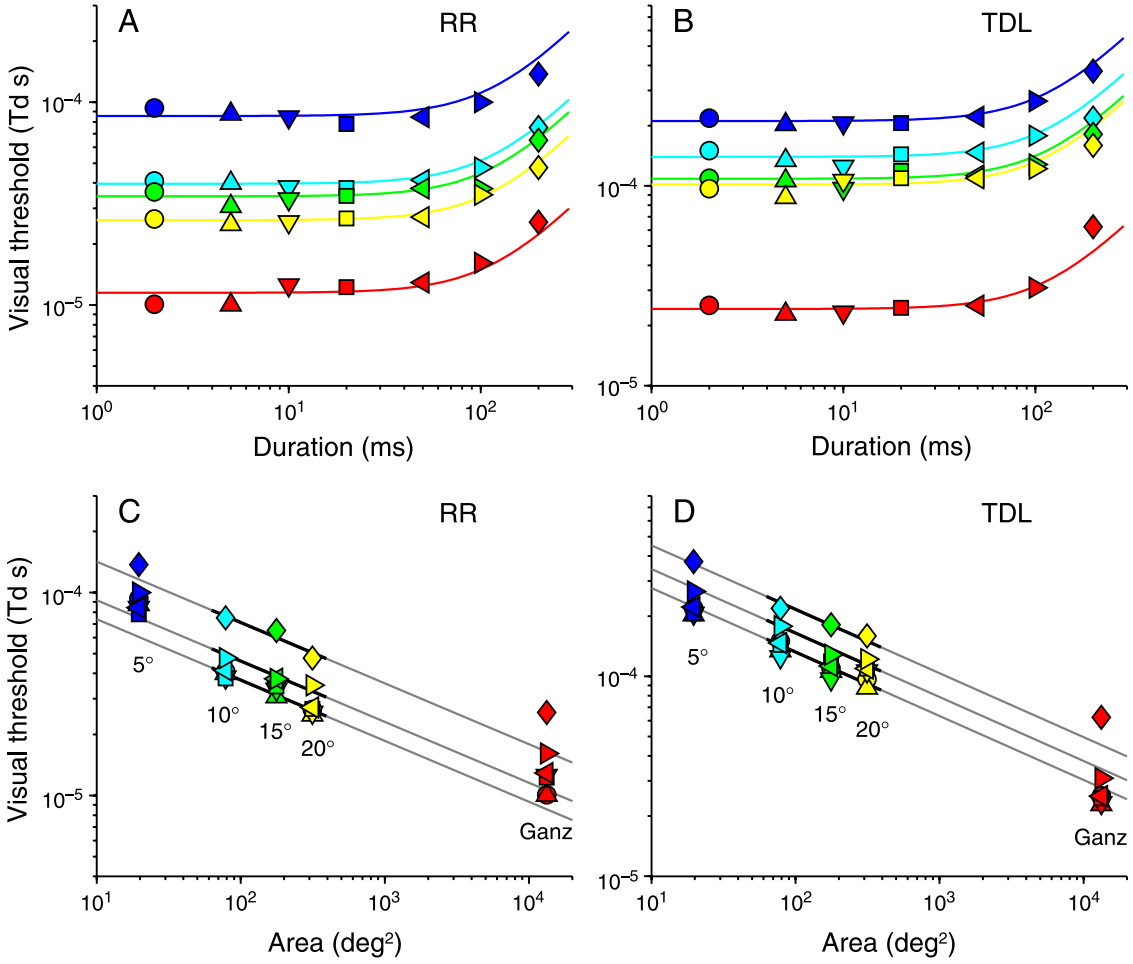

Figure 2. Dark-adapted (i.e., absolute) visual threshold. Top row: Plotted as a function of flash duration (ms). Bottom row: Plotted as a function of stimulus area (deg^2); full-field measurements are plotted at a nominal stimulus area of 13,000 deg^2 (or diameter of 130°; see text). For all panels, the stimulus duration is denoted by symbols [2 ms (○), 5 ms (△), 10 ms (▽), 20 ms (□), 50 ms (◁), 100 ms (▷), 200 ms (◇)], while the stimulus size is denoted by color and by annotation near the symbols (5°, blue; 10°, cyan; 15°, green; 20°, yellow; full field, red). Left column: Subject R.R. Right column: Subject T.D.L. The curves in the upper row asymptote to a slope of +1 at long durations, from a critical integration duration of 120 ms. The lines in the lower row have slopes of (C) −0.30 and (D) −0.32 and have been positioned vertically through the measurements over stimulus diameters of 10–20° (black lines); the bottom line is for all durations up to 50 ms.

about 0.5 deg^2 (or for diameters less than about 0.8°), considerably smaller than those studied here. The straight lines are drawn with a slope of ca. −0.3; these were positioned vertically for test stimuli in the range of 10°–20° (shown by the black lines). A slope of ca. −1/3 in these coordinates indicates that the threshold varies approximately inversely as the cube root of the area, possibly a reflection of "probability summation."

Effect of stimulus size and duration on post-bleach recovery of visual threshold

In light of our dark-adapted threshold measurements in Figure 2, we chose a restricted set of stimulus configurations with which to test post-bleach recovery of psychophysical threshold, following a nominal bleach level of 25%. We chose diameters of 5°, 20°, and full field and durations of 2 ms and 50 ms. In the dark adaptation experiments of Figure 3, these stimuli were combined in four configurations: 5°/2 ms, 5°/50 ms, 20°/2 ms, and full field/2 ms. The experiments were conducted on the same two subjects whose data are shown in Figure 2.

We interpret the measurements of post-bleach psychophysical threshold plotted for the two subjects in Figure 3 as follows. First, the fully dark-adapted thresholds (prior to bleach delivery) conform closely with the expectations from Figure 2. Thus, the dark-adapted thresholds for the two 5° diameter stimuli are very similar (at around 10^{-4} Td s), while those for the 20° and full-field stimuli are roughly 0.5 and 1 log units lower. Second, the post-bleach recoveries obtained using the three circular patch stimuli appear to be indistinguishable from each other, once account is taken of the slight vertical shift in the dark-adapted thresholds between the 5° and 20° stimuli (and with allowance for a small amount of noise in the

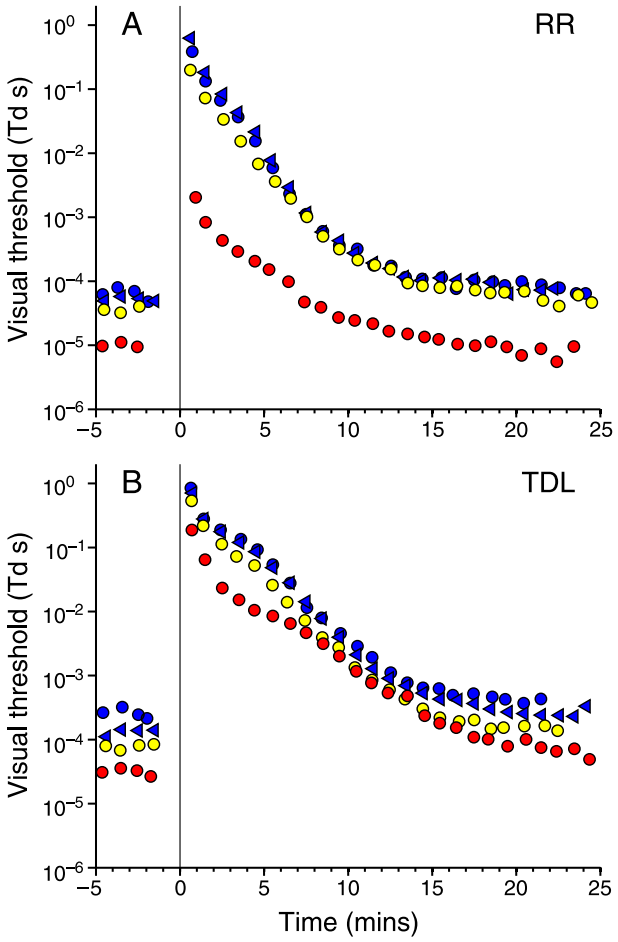

Figure 3. Post-bleach recovery of visual threshold following a bleach of ~25%, monitored with flash stimuli of various configurations. In (A) and (B), i.e., subjects R.R. and T.D.L., respectively, test spot diameters and durations are indicated using the same symbols and colors as in Figure 2 [5°/50 ms (◀), 5°/2 ms (●), 20°/2 ms (●), full field/2 ms (●)]. Points represent measurements obtained over consecutive intervals of 1 min and were averaged from up to four repetitions of the experiment (obtained in 1–4 sessions).

measurements). Third, the recovery obtained with full-field (ganzfeld) stimulation shows some discrepancy from the simple vertical shift that might be expected from the shift in dark-adapted level.

It is worth noting that each of the subjects found the experiments with full-field stimuli more demanding than those with circular patch stimuli, in part because it was not always clear where in the visual field the flash was seen. At early times after bleach extinction, though, all subjects reported that the test flashes were being seen in the far periphery of the visual field. We think that this is most likely explained by non-uniform (i.e., lower) bleaching in the far periphery. During delivery of the intense bleaching illumination, it was difficult for the subjects to avoid partial eyelid closure, which had the consequence of partly obscuring the most peripheral parts of the visual field. Furthermore, during the bleaching exposures, the subjects were asked to move their eyes around, rather than fixate, and this may also have led to a reduction in peripheral bleach levels. As a result of these factors, it seems likely that the extent of bleaching in the most peripheral regions was somewhat lower than obtained over the majority of the visual field.

Would this have affected the ERG recordings? Probably slightly, though we think not in a major way. Our impression (based mainly on the subjective nature of the apparent location of the flash at early times post-bleach) was that the region of lowered bleach level was restricted to a narrow annulus in the far periphery. As a result, only a relatively small proportion of the total retinal area contributing to the scotopic ERG signal (Holopigian, Seiple, Greenstein, Hood, & Carr, 2001; Hood et al., 1998) would have come from the region that experienced a lower level of bleach.

Our conclusion from the experiments of Figure 3, in conjunction with those of Figure 2, is that for both subjects tested with a variety of stimulus configurations following bleaches of 25%, the measured recovery was fundamentally the same for each of the patch configurations (5° and 20°, 2 ms and 20 ms), and that the recovery with full-field stimuli would have been likely to have been the same, had it not been for an unavoidable difficulty in achieving complete uniformity of bleaching out to the far periphery.

Psychophysical light adaptation under the same conditions as for dark adaptation

In order to convert the measured post-bleach psychophysical thresholds into "equivalent background intensities" by means of a Crawford transformation (Crawford, 1947), we first needed to measure each subject's light adaptation behavior under identical conditions to the dark adaptation experiments. Figure 4 illustrates the dependence of visual threshold on background intensity over the range of $<10^{-4}$ to $\sim 10^{4}$ scotopic Td, for subject T.D.L. Two configurations of patch stimulation have been plotted (5°/50 ms and 20°/2 ms); we also examined ganzfeld stimulation, but these results are not shown due to our interpretation that the full-field dark adaptation measurements (Figure 3) were affected by non-uniform bleaching in the far periphery. Psychophysical light adaptation using ganzfeld stimuli has previously been studied by Frishman et al. (1996).

The threshold measurements in both panels of Figure 4 showed clear evidence of scotopic and photopic components, described by Weber law curves of the following form:

$$\frac{s}{s_D} = 1 + \left(\frac{I}{I_s}\right)^{n_s}, \text{ and } \frac{p}{p_D} = 1 + \left(\frac{I}{I_p}\right)^{n_p}, \quad (1)$$

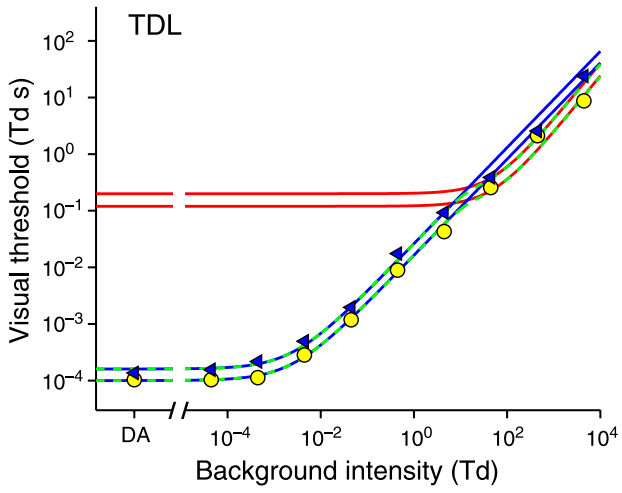

Figure 4. Light adaptation measured with test spots of two configurations [5°/50 ms (◀), 20°/2 ms (●)] collected in a single experimental session with subject T.D.L. The blue and red curves plot Equation 1, using the parameter values listed in Table 1 for this subject. The dashed green curve (which is plotted in front of the blue and red curves) represents Equation 2 using m = 4.

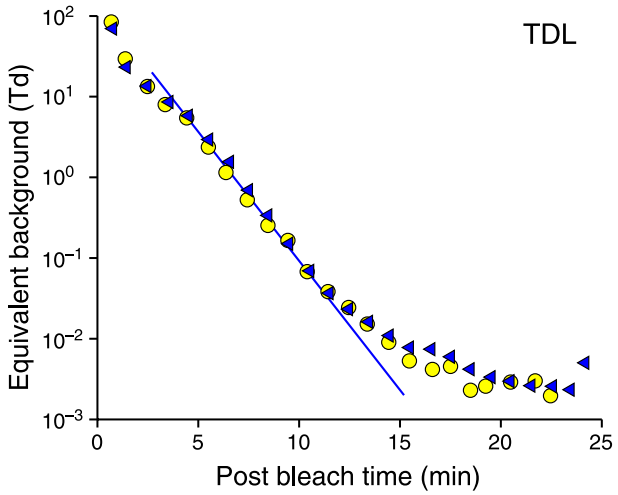

Figure 5. Equivalent background intensities derived from the measurements obtained with the two test spot configurations shown in Figure 4 [5°/50 ms (◀), 20°/2 ms (●)], using Crawford transformation via the scotopic curves fitted in Figure 4 (which are based on the parameters in Table 1). Thus, Equation 3, derived as the inverse of the first term in Equation 1, has been used to transform the measurements from Figure 4. The straight line indicates the second component of recovery, S2, drawn with a slope of −0.32 decade min^{-1} for subject T.D.L. Points above ~10 Td are in the photopic range, while points below ~10^{-2} Td correspond to the third component, S3.

respectively. Here, s and p are the scotopic and photopic thresholds, s_D and p_D are their dark-adapted values, I is the background intensity, I_s and I_p are the scotopic and photopic dark light, and n_s and n_p are the scotopic and photopic Weber law exponents. (Note that, because the intensity and threshold have been measured in scotopic units, the values of the photopic dark light (I_p) and the photopic thresholds (p and p_D) in photopic units would be lower, by a factor that we estimate to be ~1.2 log units.)

Sensory detection by independent mechanisms is conventionally accounted for in terms of probability summation, whereby the overall threshold θ is given by the power law sum:

$$\theta = (s^{-m} + p^{-m})^{-1/m}, \quad (2)$$

where the exponent is usually set to m = 4 (see Pianta & Kalloniatis, 2000).

Over most of the intensity range in Figure 4 (i.e., for backgrounds up to about 10 Td), the threshold is set by scotopic detection. The average parameter values used in fitting Equations 1 and 2 for each of the four subjects are listed in Table 1.

In addition to the Weber law fitting specified in Equation 1, we also applied fitting using a "Rose–DeVries" square-root law in addition to a Weber component in the scotopic region. Although this approach provided a marginally better description in the region of 10^{-3}–10^{-2} Td (not shown), we did not regard the slight improvement as justifying the additional arbitrary parameters required.

Conversion to equivalent background intensity: Crawford transformation

Figure 5 plots the decay of equivalent background intensity for the experiments in Figure 3, upon Crawford

		Weber law (Equation 1)					
		s_D (Td s)	I_s (Td)	n_s	p_D (Td s)	I_p (Td)	n_p
T.D.L.	5°/50 ms	1.6×10^{-4}	2.5×10^{-3}	0.85	0.2	50	1
	20°/2 ms	1×10^{-4}	2.5×10^{-3}	0.85	0.12	50	1
R.R.	5°/50 ms	8.8×10^{-5}	4×10^{-3}	0.9	0.2	100	1
M.J.P.	5°/50 ms	1.4×10^{-4}	5×10^{-3}	0.9	0.15	100	1
A.M.C.	5°/50 ms	1.1×10^{-4}	6×10^{-4}	0.9	0.1	20	1

Table 1. Summary of fitted parameter values for psychophysical light adaptation, for the four subjects.

transformation using the scotopic light adaptation results in Figure 4. Thus, the inverse of the scotopic curve (such as the blue curves fitted in Figure 4) given by

$$I_{\text{equiv}} = I_{\text{s}}\left(\frac{s}{s_{\text{D}}} - 1\right)^{1/n_{\text{s}}}, \quad (3)$$

was used to convert the corresponding visual threshold data from Figure 3 into equivalent background intensity.

Importantly, the data points in Figure 5 demonstrate that the extracted decay of equivalent background intensity is common, irrespective of the stimulus configuration (for these two configurations, using 5°/50 ms and 20°/2 ms test stimuli). Given that the derived values of equivalent background intensity were similar, regardless of stimulus patch size, we decided to standardize on a 5°/50 ms test stimulus for all subsequent psychophysical experiments.

Our presumption is that, had it been possible to achieve uniform bleaching over the entire retina, then for each subject the recovery of equivalent background intensity using ganzfeld stimuli would have conformed to the common recovery obtained with circular patch stimuli.

Post-bleach recovery of visual threshold after bleaches of different size

Figure 6A plots psychophysical dark adaptation obtained from one subject (M.J.P.), for multiple presentations of bleaches at seven levels, ranging from around 1% to near total (Table 2). Each bleach level is represented by a separate color, and in each case, the experiment was repeated on three occasions (indicated by the three sets of symbols: ○, ◇, △). For each bleaching level, the three recoveries were broadly consistent, though some differences are noticeable. For example, following the largest bleach (indicated by the open symbols), the triangles (△) appear to be delayed by roughly 1 min from the other two sets of symbols. Horizontal shifts of this kind are likely to be accounted for by small differences in the level of bleaching achieved, while vertical shifts (at least in the pre-bleach threshold) might be explained by factors such as diurnal rhythms.

Following delivery of the largest bleach (~90%), the subject's visual threshold was initially elevated by more than 4 log units, and then recovered with a characteristic biphasic form. The initial phase of recovery, known to be mediated by the cone system, occurred rapidly and reached a plateau level of ~0.08 Td s. The rod–cone break was reached at 12 min, after which rod-mediated recovery occurred steadily for the next 10 min and thereafter occurred very slowly.

The family of post-bleach dark adaptation recoveries illustrated in Figure 6A is typical of those we recorded for the four subjects. Results from a second subject (T.D.L.)

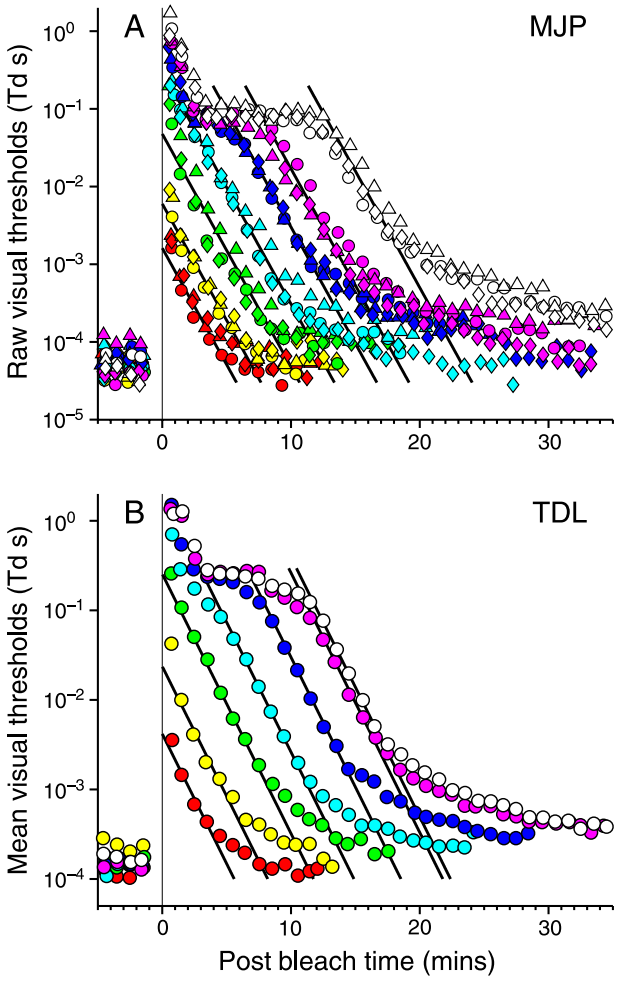

Figure 6. Recovery of visual threshold following a range of bleaching strengths. The bleaches, nominally of seven magnitudes (1%, 4%, 12%, 25%, 50%, 70%, and 85%), are indicated using the symbol color scheme shown in Table 3. All measurements were obtained using 5°/50 ms flash stimuli. (A) Results from individual experiments for subject M.J.P. Three repetitions of measurements at each bleaching strength are shown; each strength is indicated using different colors. (B) Mean results for the seven bleaching levels for subject T.D.L. (averaged from up to 3 repetitions). The parallel straight lines plot the S2 component of recovery: (A) −0.30 and (B) −0.29 $\log_{10}$ unit min^{-1}.

are plotted in Figure 6B, in this case after averaging across the measurements from 2 or 3 repetitions of each bleaching level.

These recoveries are very similar in form to those reported in previous studies for normal subjects, for example, in Cideciyan et al. (1997, Figure 1A); Hecht, Haig, and Chase (1937, Figure 2); Jacobson et al. (1996, Figure 4); and Pugh (1975, Figures 1 and 3). For the extensive data of Pugh, replotted in Lamb and Pugh (2004, Figure 6), the test stimulus was a circular patch 1.9° in diameter, centered 13.4° in the temporal parafovea, 55 ms in duration, and of dominant wavelength 450 nm,

		Psychophysical experiments Nominal bleach levels						
		~1%	~4%	~12%	~25%	~50%	~70%	~85%
		●	●	●	●	●	●	○
TDL	$\times 10^6$ Td s	0.069	0.22	0.68	1.5	3.0	5.5	9.9
	B	1.3%	4.0%	12%	25%	44%	65%	84%
RR	$\times 10^6$ Td s	0.070	0.25	0.75	1.5	3.2	6.6	8.6
	B	1.3%	4.6%	13%	24%	47%	71%	81%
MJP	$\times 10^6$ Td s	0.062	0.19	0.65	1.5	3.0	5.4	13
	B	1.2%	3.5%	11%	25%	43%	65%	91%
AMC	$\times 10^6$ Td s	0.066	0.20	0.65	1.3	3.8	6.4	11
	B	1.3%	3.7%	11%	22%	51%	71%	87%

Table 2. Psychophysical experiments. Actual average bleach intensity-time products delivered (Td s) and calculated bleach levels (%), for each subject and for the various nominal bleaches. Symbols denote those used in Figure 6 and in the left column of Figure 7.

and the bleaches delivered from 4.7 to 7.6 log scotopic Td s over a field 23.5° in diameter.

Over a substantial region, the psychophysical dark adaptation recoveries in Figure 6 decline with constant slope in these semi-logarithmic coordinates. This behavior has been reported previously for other normal subjects (Lamb, 1981, 1990; Lamb & Pugh, 2004; Owsley et al., 2001) and is referred to as the "S2" component of dark adaptation; this appears to be a characteristic feature of psychophysical dark adaptation measurements. In Figures 6A and 6B, the parallel straight lines for the two subjects are drawn with slopes of −0.30 (M.J.P.) and −0.29 (T.D.L.) $\log_{10}$ unit min^{-1}, respectively, consistent with the population range reported by Jackson et al. (1999, Figure 2B).

At late times, the recovery was slower than predicted by the S2 component and exhibited an additional "S3" component, as described by Lamb (1981), with a slope of roughly −0.05 $\log_{10}$ unit min^{-1}. In the next figure, we fit both the S2 and S3 components.

Comparison of post-bleach equivalent background intensities estimated from psychophysical thresholds and from ERG *b*-waves

In Figure 7, we compare the post-bleach recoveries of equivalent background intensity for our four subjects, calculated both from the psychophysical measurements (left column) and from the ERG *b*-wave measurements (right column). The bleach levels are color-coded, as indicated in Table 2 for the psychophysical experiments and in Table 3 for the ERG experiments.

In both cases, the raw post-bleach measurements have been transformed into equivalent background intensities using the inverse of the measured light adaptation function (i.e., by Crawford transformation), as described in relation to Figure 5 for the psychophysical measurements and in Cameron et al. (2006, 2008) for the ERG *b*-wave measurements.

For subjects T.D.L. and A.M.C., the *b*-waves were measured using a test flash of constant intensity (Cameron et al., 2006), and the resulting Weber law exponent *n* was relatively low, at 0.74 and 0.80. For subjects R.R. and M.J.P., the test flash intensity was adjusted so as to yield an approximately constant response amplitude (Cameron et al., 2008), and the exponent *n* was then closer to unity, at 0.9 and 0.94.

As a check, we also applied Crawford transformation of the psychophysical results based on inversion of the light adaptation measurements fitted by the combination of a Rose–DeVries square-root region as well as a Weber region; the resulting recoveries of equivalent background (not shown) were barely distinguishable from those obtained using only the Weber approach.

In each panel of Figure 7, we have plotted curves representing the sum of two exponentially decaying components of equivalent background, S2 and S3, according to the following equation:

$$I_{\text{equiv}}(t) = I_{\text{S2}}(0)10^{-\Psi_{\text{S2}}t} + I_{\text{S3}}(0)10^{-\Psi_{\text{S3}}t}, \quad (4)$$

where Ψ_{S2} and Ψ_{S3} are the slopes of the S2 and S3 components in $\log_{10}$ units min^{-1}, and $I_{\text{S2}}(0)$ and $I_{\text{S3}}(0)$ are the initial magnitudes of the S2 and S3 components at extinction of the bleaching light. (Note that we do not need to include the absolute dark light, as the Crawford transform in Equation 3 extracts the equivalent background in excess of the absolute dark light.)

In order to estimate values for the four parameters in each panel, we used least-squares regression to fit

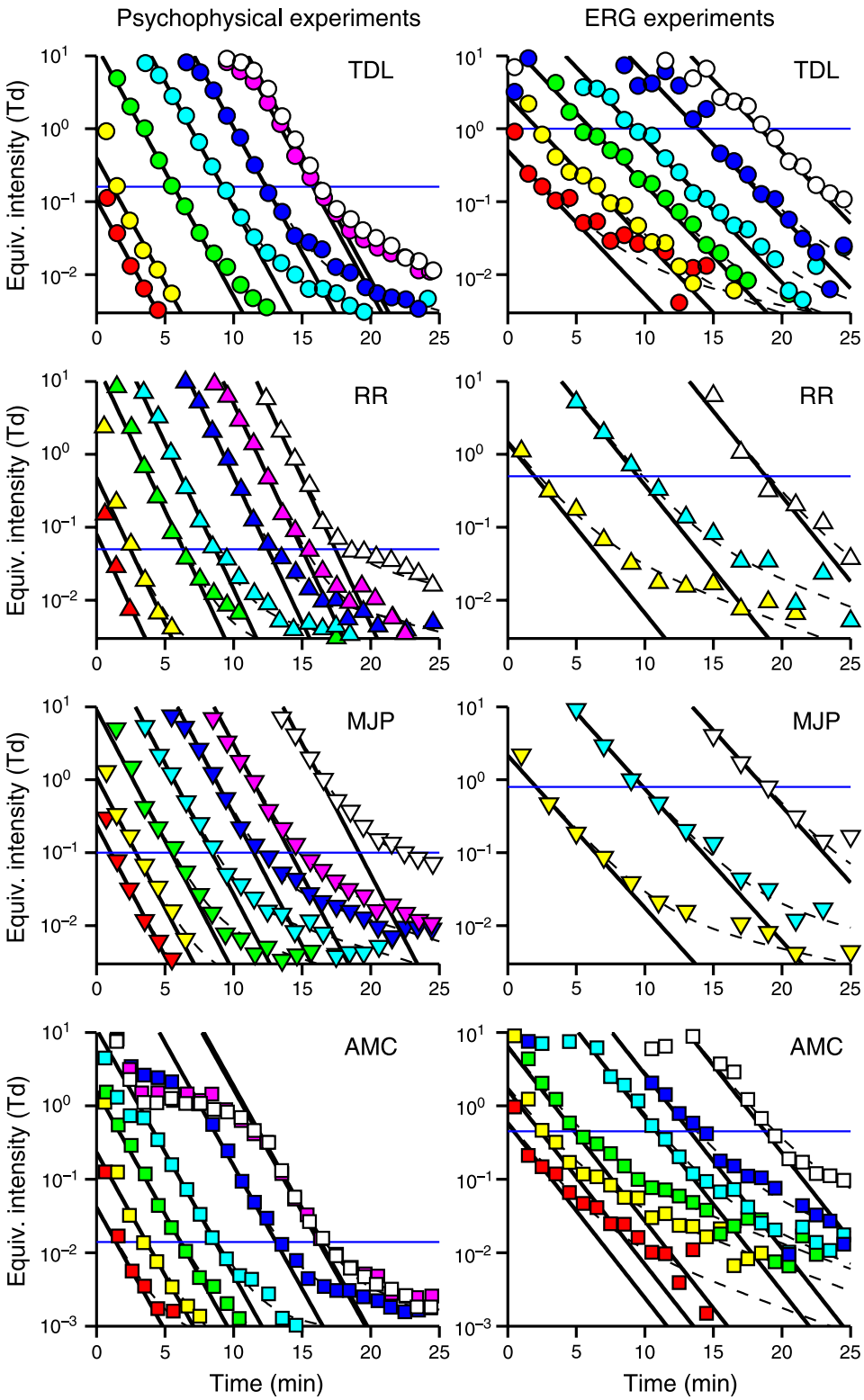

Figure 7. Post-bleach decline of equivalent background intensities for the four subjects. Left column: "Threshold-equivalent background". Right column: "ERG-equivalent background." Both sets of results have been fitted with the sum of "S2" and "S3" components (dashed curves), according to Equation 4, with slopes given in Table 4; the "S2" components are shown by the thick lines. The subjects are identified by different symbols that are also used in the next two figures. The colors indicate average bleach strength as indicated in Tables 2 (psychophysical) and 3 (ERG) and again in the next two figures. All vertical scales are common, except those for A.M.C., which extend an additional 3× lower. Horizontal blue lines are used for deriving Figure 9.

		ERG experiments Nominal bleach levels					
		~2%	~6%	~14%	~30%	~50%	~95%
		●	●	●	●	●	○
TDL	$\times 10^6$ Td s	0.10	0.36	0.86	1.8	4.1	18
	B	1.9%	6.5%	15%	30%	56%	96%
RR	$\times 10^6$ Td s		0.35		1.7		21
	B		6.3%		28%		96%
MJP	$\times 10^6$ Td s		0.33		1.9		17
	B		6.1%		30%		93%
AMC	$\times 10^6$ Td s	0.13	0.37	0.7	2.0	3.9	23
	B	2.3%	6.7%	13%	31%	53%	98%

Table 3. ERG experiments. Actual average bleach intensity-time products delivered (Td s) and calculated bleach levels (%), for each subject and for the various nominal bleaches. Symbols denote those used in the right column of Figure 7.

Equation 4 to the complete set of recoveries in that panel; the values for Ψ_{S2} and Ψ_{S3} were yolked across all bleach levels within a panel, while $I_{S2}(0)$ and $I_{S3}(0)$ were allowed to vary for the individual bleach levels. Using this approach, it was possible to obtain a good fit to the set of recoveries in each panel in Figure 7 using Equation 4.

In the left column of Figure 7, the post-bleach equivalent background intensity derived from visual thresholds shows a clear S2 component for each subject and for each bleach level. For the two subjects (M.J.P. and T.D.L.) whose data were plotted as visual thresholds in Figure 6, the slopes are somewhat higher in the left panel of Figure 7, because the Weber law exponent for the psychophysical light adaptation measurements (Figure 4) was less than unity (0.85–0.9) for each subject. In the right-hand column of Figure 7, the post-bleach equivalent background intensities calculated from the ERG *b*-wave recordings likewise display a clear S2 component of recovery, though with a shallower slope than in the left column.

The slopes of the S2 and S3 components plotted in Figure 7 are given in Table 4 for each of the subjects, for both the psychophysical and ERG experiments. Across the four subjects, the mean S2 slopes, Ψ_{S2}, were -0.359 (psychophysical) and -0.219 (ERG) $\log_{10}$ unit min^{-1}, indicating that the S2 slope was around 60% higher in the psychophysical experiments than in the ERG experiments. In the Conclusions section, we will address the likely reasons for this difference.

The recoveries of post-bleach equivalent background intensity calculated from the psychophysical measurements and from the ERG *b*-wave measurements are compared in Figure 8 for the four subjects at a representative bleach level (25–30%). Thus, the results have been replotted from all the cyan measurements in Figure 7.

The curves show fits (obtained by eye) for the S2 and S3 components of recovery, averaged across the four subjects, for the psychophysical measurements (upper curve) and for the ERG measurements (lower curve). For these manual fits, the slope of the S2 component is roughly 36% greater when determined from the psychophysical measurements than when determined from the ERG *b*-wave measurements.

Dependence of recovery time on bleach level

Figure 9 plots the dependence of post-bleach recovery time on the magnitude of the bleach. For each subject, we chose a criterion level of equivalent background within the S2 region of recovery (shown by the dashed horizontal blue lines in Figure 7), and we measured the time taken

Parameters in Figure 7	TDL	RR	MJP	AMC
Psychophysical				
Ψ_{S2}, S2 slope ($\log_{10}$/min)	−0.34	−0.40	−0.36	−0.34
Ψ_{S3}, S3 slope ($\log_{10}$/min)	−0.05	−0.05	−0.06	−0.03
Criterion I_{equiv} (Td)	0.16	0.05	0.1	0.014
ERG				
Ψ_{S2}, S2 slope ($\log_{10}$/min)	−0.20	−0.23	−0.21	−0.24
Ψ_{S3}, S3 slope ($\log_{10}$/min)	−0.04	−0.07	−0.04	−0.07
Criterion I_{equiv} (Td)	1	0.5	0.8	0.45

Table 4. Parameters Ψ_{S2} and Ψ_{S3} in Equation 4, describing the slopes of the S2 and S3 components of decay of the "psychophysical threshold equivalent" and "ERG desensitization equivalent" background intensities, as plotted by the curves in Figure 7. The criterion levels of background intensity are those plotted as horizontal dashed lines in Figure 7 and used subsequently in plotting Figure 9.

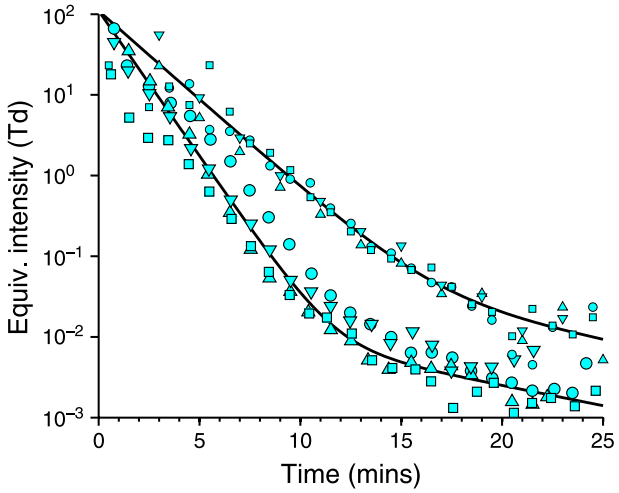

Figure 8. Comparison of "threshold equivalent background" and "ERG equivalent background" intensities following bleaches of 25–30%; measurements are taken from cyan symbols in Figure 7. Larger symbols plot psychophysical threshold equivalent intensities, while smaller symbols plot ERG equivalent intensities: T.D.L. (○), R.R. (△), M.J.P. (▽), A.M.C. (□). The psychophysical measurements for A.M.C. have been scaled vertically by 4×. Curves plot Equation 4 with Ψ_{S2} and Ψ_{S3} set to the mean observed values of −0.36 and −0.05 (psychophysical) and −0.22 and −0.05 (ERG) $\log_{10}$ unit min^{-1}.

for the S2 component to reach this level for each bleach. Varying the level of the criterion background intensity simply causes a left–right shift in the set of crossing times, because the recoveries are parallel in the S2 region. In order to allow for inter-subject variability, we set the criterion intensity for each subject at a level that shifted the sets of points in Figure 9 to achieve conformity between subjects.

According to the "MLP" analysis and modeling of Lamb and Pugh (2004) and Mahroo and Lamb (2004), the decay of the S2 component of equivalent background reflects the disappearance of opsin (bleached rhodopsin) in rods by combination with 11-*cis* retinal to re-form rhodopsin. A theoretical expression for the time t taken to reach a criterion level of recovery was derived by Mahroo and Lamb (2004) as their Equation A17:

$$t = \frac{(B - \text{Ops}) - K_m \ln(\text{Ops}/B)}{(1 + K_m)v}. \quad (5)$$

As previously, B is the level of bleach at extinction of the illumination, and v and K_m are the limiting rate and semi-saturation constant of regeneration. In addition, Ops is the criterion fraction of free opsin for which the time t is being calculated to; however, this is a dummy parameter, and changing its level simply causes a left–right shift in the relation between recovery time t and bleach level B (in just the same way that varying the criterion level of equivalent background intensity in Figure 7 causes a left–right shift in the measured recovery times in Figure 9).

The prediction of Equation 5 is plotted as the curve in Figure 9 and provides a good fit to the points extracted from both the threshold equivalent and ERG equivalent background intensities, using the same parameters for the limiting rate (v = 0.084 min^{-1}) and semi-saturation constant (K_m = 0.18) as used to calculate the bleach levels in Tables 2 and 3 (see Methods section).

Conclusions

We begin by evaluating potential limitations in our experimental approach, and thereafter, we present the interpretations that we can make from the results that we obtained.

Potential limitations in the experiments

Bleach magnitudes

We suspect that there may have been inadvertent errors in the calculated magnitudes of some of the bleaching exposures, especially for very large bleaches. These

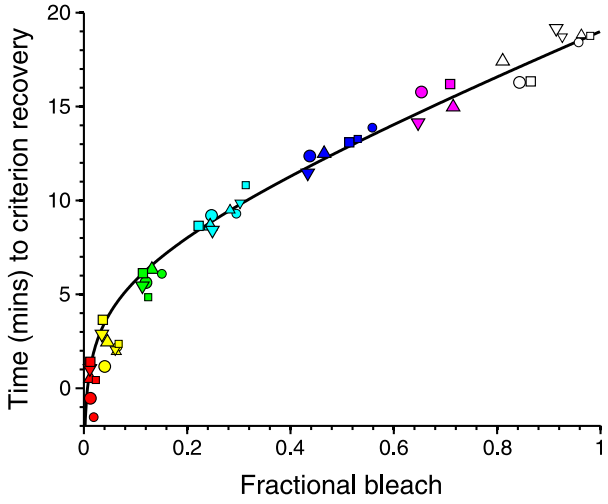

Figure 9. Plot of the time taken for the S2 component of equivalent background to reach a criterion level of background intensity. The criterion levels chosen are indicated by the horizontal blue lines in Figure 7 and are given in Table 4. The ordinate plots the times of the intercept of the S2 component straight lines in Figure 7 with the criterion level for that panel. Color-coding denotes the bleach level according to Tables 2 and 3 and Figure 7. Larger symbols plot threshold equivalent measurements, while smaller symbols plot ERG equivalent measurements: T.D.L. (○), R.R. (△), M.J.P. (▽), A.M.C. (□). The curve plots the prediction of the MLP rate-limited model for the disappearance of free opsin, as given by Equation 5, with our standard values of v = 0.084 min^{-1} and K_m = 0.18.

intense and lengthy ganzfeld exposures proved difficult for the subjects to endure, and there was inevitable involuntary blinking and partial eyelid closure. Although we used a video camera to monitor the eye during the exposures, we may not have compensated fully for lowered light entry. Thus, in Figure 7, it is apparent in the left column that the two largest bleaches (magenta and white symbols) gave quite similar recoveries for subjects T.D.L. and A.M.C., yet quite different recoveries for subject M.J.P. We think that this must reflect error(s) in the estimation of these bleach levels.

Psychophysical experiments: Avoidance of ganzfeld stimuli

In order for ERG measurements to be most easily interpreted, the stimuli need to be ganzfeld, so that the photoreceptors across the entire retina receive the same intensity of illumination. However, for the psychophysical experiments, there were practical difficulties in using ganzfeld test stimuli. First, it was not feasible to achieve bleaching that was completely uniform right out to the far periphery, because of a combination of deliberate eye movements made during the bleach delivery and involuntary partial eyelid closure during the bleaches. Second, subjects typically found it quite frustrating trying to make the psychophysical threshold measurements with ganzfeld stimuli, perhaps because the flash could appear to occur anywhere in the visual field. As a result, we chose to make the ERG measurements with ganzfeld stimuli and to make the psychophysical measurements with stimuli of finite area. We, therefore, needed to test the comparability of the measurements using the two approaches.

Psychophysical experiments: Appropriateness of using stimuli of finite area

We began by investigating the effects of stimulus size and duration on the psychophysical measurements obtained under dark-adapted conditions, and then we examined certain combinations of flash duration and stimulus size in light adaptation and dark adaptation experiments.

Under dark-adapted conditions, we found complete temporal summation for stimulus durations up to at least 50 ms (Figures 2A and 2B); thus, at visual threshold, the quantity of light (in Td s) was invariant with flash duration up to 50 ms. Spatial summation was partial, for the tested stimulus sizes from 5° in diameter to ganzfeld, with visual threshold varying inversely as approximately the cube root of the stimulus area (Figures 2C and 2D), presumably a reflection of probability summation.

In light adaptation experiments, we found very similar behavior when using either a small area longer duration (5°/50 ms) stimulus or a larger area short duration (20°/2 ms) stimulus (Figure 4). In dark adaptation experiments following a representative bleach (of 25%), the recovery was very similar when measured using the above two stimulus configurations (see Figure 3, in units of visual threshold, and Figure 5, after conversion to equivalent background intensity).

From these results, we conclude that the stimulus parameters are not critical in estimating the post-bleach equivalent background intensity in psychophysical experiments and that a 5°/50 ms stimulus provided estimates of the decay of equivalent background intensity that would have conformed to those that would have been obtained with a ganzfeld stimulus, had it been possible to deliver spatially uniform ganzfeld bleaches. Hence, these results should be appropriate for comparison with the estimates of equivalent background obtained in the ERG experiments.

ERG experiments: Magnitudes of flash and background intensities

One considerable difference between the two sets of experiments relates to the magnitudes of the intensities of the test and adapting stimuli. For the ERG experiments, the test flash intensities were around 1000 times higher than for psychophysical threshold, e.g., 0.03–0.1 Td s for the ERG experiments versus $\sim 3 \times 10^{-5}$ Td s for the psychophysical experiments (in both cases using ganzfeld stimuli under dark-adapted conditions). Likewise, the adapting intensities and the dark light were typically 20–100 times higher, e.g., a dark light of ~0.2 Td for the ERG scotopic *b*-wave but $2–5 \times 10^{-3}$ Td for the scotopic threshold.

We cannot rule out the possibility that the necessity, in the ERG experiments, of using flash and steady intensities far above psychophysical threshold and psychophysical dark light may have affected the estimation of equivalent background intensity. However, in our previous study, we did not detect any obvious effect of flash intensity (0.02 and 0.1 Td s) on the recovery of the calculated equivalent background for subject A.M.C. (Cameron et al., 2006). Nevertheless, it is conceivable that the vertical scaling of the estimated equivalent background intensity in the ERG experiments is not reliable and that the slope of the S2 component determined from the ERG experiments might have been underestimated (see below).

Comparison of post-bleach recovery for psychophysical and ERG experiments

In Figure 7, the decline of "threshold-equivalent" background intensity (left column) exhibited broadly similar kinetics to the decline of "ERG-equivalent" background intensity (right column). In each case, the equivalent background declined for much of its range with a prominent S2 component of recovery, and in addition, this component exhibited a rightward shift with increasing bleach level. A substantial body of evidence

indicates that the slope and the lateral shifting of the S2 component are both indicators of the decline in the amount of free opsin (bleached rhodopsin) in the rod outer segments, as opsin is reconverted to rhodopsin by combination with 11-*cis* retinal (see Lamb & Pugh, 2004). The lateral shifting seen with larger bleaches provides a measure of the "rate-limited" decline of free opsin when its level is high (see below), whereas the fixed slope seen at late stages provides a measure of the final exponential decline in free opsin when its level is very low.

Rate-limited recovery of opsin following relatively large bleaches

The lateral time shifting of the S2 region of recovery with increasing bleach magnitude was comparable, when determined from psychophysics or from ERGs. Thus, in Figure 7, the time for the "threshold-equivalent" background to reach a criterion level of ~0.05 Td resembles the time required for the "ERG-equivalent" background to reach a level of ~0.5 Td.

For both approaches, the relationship between recovery time and bleach level (plotted in Figure 9) is well described by the predictions of a theoretical model that describes the decline in opsin level as a function of time. The extracted time course of decline in opsin level may be visualized more intuitively by rotating Figure 9 counterclockwise by 90°, whereupon the new "vertical" axis provides a measure of the remaining opsin level while the new "horizontal" axis represents increasing time to the right (see Lamb & Pugh, 2004). It can then be seen that the decline in opsin level is initially roughly linear with time, i.e., rate-limited.

We find it compelling that the two approaches (the lateral shifts of psychophysical threshold and of ERG) generate essentially the same estimates for the time course of decline of opsin level in the large bleach region, despite the finding that the extracted slope of the S2 region differed between the two approaches. This suggests that both approaches are measuring the same phenomenon, though for some reason the S2 slope determined by at least one of the approaches does not equate to the slope of the final exponential decline in opsin level.

Final exponential time course of opsin decline

The mean S2 slope (Ψ_{S2}) for equivalent background in our psychophysical experiments was -0.359 $\log_{10}$ unit min^{-1}. Although this may seem higher than values reported in the literature, the main reason for the apparent difference is that our value is for equivalent background, whereas those in the literature have been for visual threshold and will, therefore, have been scaled down from ours by the exponent of the Weber law relation in those experiments. As earlier studies typically used test stimuli of smaller diameter (e.g., 1.9°; Pugh, 1975), it is plausible that the Weber exponent in those studies may have been lower, at around 0.8. A second contributory factor is that our least-squares fitting of the sum of S2 and S3 components tended to give a marginally higher estimate of S2 slope than was obtained by simply fitting a straight line to S2 by eye.

For our four subjects, the mean S2 slope in the ERG *b*-wave experiments, -0.219 $\log_{10}$ unit min^{-1}, was around two-thirds the value above in the psychophysical experiments. However, it was close to the value obtained previously in ERG *a*-wave experiments for the S2 slope of equivalent background, of around -0.2 $\log_{10}$ unit min^{-1} (Thomas & Lamb, 1999). Likewise, the vertical scaling of the equivalent intensity was similar in the *a*-wave and *b*-wave experiments.

Mechanistically, the time course of the decay of the S2 product must be the same, no matter how it is determined. Hence, the differences in S2 slope for the equivalent background estimated by the psychophysical and ERG approaches would seem most likely to indicate some kind of discrepancy in the conversion to equivalent background between the two approaches. Ideally, we would wish to measure opsin levels directly, but we know of no suitable method. Retinal densitometry is able to measure rhodopsin levels, but it cannot directly measure opsin (as it is transparent), and subtraction is particularly problematical in the S2 region of interest, where opsin levels are low (e.g., below 1%). Densitometric measurements from the literature, plotted in Figure 10 of Lamb and Pugh (2004), are consistent with an S2 slope for equivalent background (calculated as $v\ (1 + K_m) / 2.303K_m$) in the range of 0.22–0.39 min^{-1}.

We do not have a complete explanation for the discrepancy in our estimates of S2 slope, but we think that it is most likely to result from a significant underestimation of the true slope by the ERG approach. This may have occurred in part because of non-linearities that resulted from the need to use much higher test flash intensities in the ERG experiments than in the threshold experiments and in part because the intensities required to adapt the ERG response were also much higher. In addition, in fitting the Weber curves to the ERG light adaptation results, we chose to fix the Weber exponent during curve fitting because the exponent was not well constrained, and it is possible that this might have influenced our estimate of the ERG S2 slope. There are no obvious factors that might have caused overestimation of the S2 slope in the psychophysical experiments, given that the Weber exponent for the thresholds was quite close to unity. For the future, it will be important to try to design experiments that resolve the present discrepancy in S2 slope determined by the two approaches.

Magnitude of the equivalent background

There was also a difference in the magnitude of the post-bleach equivalent background that we calculated for the rod bipolar cells and the overall visual system. Thus,

in order to align the measurements in Figure 9 for recovery of equivalent background to a criterion level, it was necessary to choose the criterion level (Figure 7, blue horizontal lines) to be ~1 $\log_{10}$ unit lower in the psychophysical experiments than in the ERG experiments. For real light, it is well established that a given background intensity tends to exert greater effectiveness at more central levels of visual processing (see, for example, Frishman et al., 1996; Green & Powers, 1982). Thus, our observation of a difference in intensity of equivalent background is in no way unexpected.

Summary

We conclude that our psychophysical measurements and our ERG *b*-wave measurements both reflect the post-bleach decline of free opsin level in the rod outer segments. The lateral shifts determined by the two approaches extract the same time course of decline when the opsin level is moderately high, but there is an unresolved discrepancy between the two approaches in estimating the final exponential rate of recovery when the opsin level is low.

Acknowledgments

This research was supported by the Australian Research Council through the ARC Centre of Excellence in Vision Science (CE0561903).

Commercial relationships: none.
Corresponding author: Trevor D. Lamb.
Email: Trevor.Lamb@anu.edu.au.
Address: John Curtin School of Medical Research, The Australian National University, Canberra, Australia.

References

Barlow, H. B. (1958). Temporal and spatial summation in human vision at different background intensities. *The Journal of Physiology, 141,* 337–350.

Barlow, H. B. (1972). Dark and light adaptation: Psychophysics. In D. Jameson & L. M. Hurvich (Eds.), *Handbook of sensory physiology* (vol. VII/4, pp. 1–28). Berlin, Germany: Springer.

Blakemore, C. B., & Rushton, W. A. H. (1965). Dark adaptation and increment threshold in a rod monochromat. *The Journal of Physiology, 181,* 612–628.

Cameron, A. M., Mahroo, O. A. R., & Lamb, T. D. (2006). Dark adaptation of human rod bipolar cells measured from the *b*-wave of the scotopic electroretinogram. *The Journal of Physiology, 575,* 507–526.

Cameron, A. M., Miao, L., Ruseckaite, R., Pianta, M. J., & Lamb, T. D. (2008). Dark adaptation recovery of human rod bipolar cell response kinetics estimated from scotopic *b*-wave measurements. *The Journal of Physiology, 586,* 5419–5436.

Cideciyan, A. V., Haeseleer, F., Fariss, R. N., Aleman, T. S., Jang, G. F., Verlinde, C. L. M. J., et al. (2000). Rod and cone visual cycle consequences of a null mutation in the 11-*cis*-retinol dehydrogenase gene in man. *Visual Neuroscience, 17,* 667–678.

Cideciyan, A. V., Pugh, E. N., Jr., Lamb, T. D., Huang, Y., & Jacobson, S. G. (1997). Rod plateaux during dark adaptation in Sorsby's fundus dystrophy and vitamin A deficiency. *Investigative Ophthalmology & Visual Science, 38,* 1786–1794.

Cornwall, M. C., & Fain, G. L. (1994). Bleached pigment activates transduction in isolated rods of the salamander retina. *The Journal of Physiology, 480,* 261–279.

Crawford, B. H. (1947). Visual adaptation in relation to brief conditioning stimuli. *Proceedings of the Royal Society of London B: Biological Sciences, 134,* 283–302.

Frishman, L. J., Reddy, M. G., & Robson, J. G. (1996). Effects of background light on the human dark-adapted electroretinogram and psychophysical threshold. *Journal of the Optical Society of America A, Optics, Image Science, and Vision, 13,* 601–612.

Green, D. G., & Powers, M. K. (1982). Mechanisms of adaptation in the rat retina. *Vision Research, 22,* 209–216.

Hecht, S., Haig, C., & Chase, A. M. (1937). The influence of light adaptation on subsequent dark adaptation of the eye. *Journal of General Physiology, 20,* 831–850.

Hecht, S., Shlaer, S., & Pirenne, M. H. (1942). Energy, quanta, and vision. *Journal of General Physiology, 25,* 819–840.

Holopigian, K., Seiple, W., Greenstein, V. C., Hood, D. C., & Carr, R. E. (2001). Local cone and rod system function in patients with retinitis pigmentosa. *Investigative Ophthalmology & Visual Science, 42,* 779–788.

Hood, D. C., Wladis, E. J., Shady, S., Holopigian, K., Li, J., & Seiple, W. (1998). Multifocal rod electroretinograms. *Investigative Ophthalmology & Visual Science, 39,* 1152–1162.

Jackson, G. R., Owsley, C., & McGwin, G. (1999). Aging and dark adaptation. *Vision Research, 39,* 3975–3982.

Jacobson, S. G., Cideciyan, A. V., Kemp, C. M., Sheffield, V. C., & Stone, E. M. (1996). Photoreceptor function in heterozygotes with insertion or deletion mutations

in the RDS gene. *Investigative Ophthalmology & Visual Science, 37,* 1662–1674.

Jacobson, S. G., Cideciyan, A. V., Regunath, G., Rodriguez, F. J., Vandenburgh, K., Sheffield, V. C., et al. (1995). Night blindness in a TIMP3-associated Sorsby's fundus dystrophy is reversed by vitamin A. *Nature Genetics, 11,* 27–32.

Jacobson, S. G., Voigt, W. J., Parel, J. M., Apáthy, P. P., Nghiem-Phu, L., Myers, S. W., et al. (1986). Automated light- and dark-adapted perimetry for evaluating retinitis pigmentosa. *Ophthalmology, 93,* 1604–1611.

Lamb, T. D. (1981). The involvement of rod photoreceptors in dark adaptation. *Vision Research, 21,* 1773–1782.

Lamb, T. D. (1990). Dark adaptation: A re-examination. In R. F. Hess, K. Nordby, & L. T. Sharpe (Eds.), *Night vision: Basic, clinical and applied aspects* (pp. 177–222). Cambridge, UK: CUP.

Lamb, T. D., & Pugh, E. N., Jr. (2004). Dark adaptation and the retinoid cycle of vision. *Progress in Retinal and Eye Research, 23,* 307–380.

Lamb, T. D., Pugh, E. N., Cideciyan, A. V., & Jacobson, S. G. (1997). A conceptual framework for analysis of dark adaptation kinetics in normal subjects and in patients with retinal disease. *Investigative Ophthalmology & Visual Science, 38,* S1121.

Leibrock, C. S., & Lamb, T. D. (1997). Effect of hydroxylamine on photon-like events during dark adaptation in toad rod photoreceptors. *The Journal of Physiology, 501,* 97–109.

Leibrock, C. S., Reuter, T., & Lamb, T. D. (1994). Dark adaptation of toad rod photoreceptors following small bleaches. *Vision Research, 34,* 2787–2800.

Mahroo, O. A. R., & Lamb, T. D. (2004). Recovery of the human photopic electroretinogram after bleaching exposures: Estimation of pigment regeneration kinetics. *The Journal of Physiology, 554,* 417–437.

Melia, T. J., Jr., Cowan, C. W., Angleson, J. K., & Wensel, T. G. (1997). A comparison of the efficiency of G protein activation by ligand-free and light-activated forms of rhodopsin. *Biophysical Journal, 73,* 3182–3191.

Nordby, K., Stabell, B., & Stabell, U. (1984). Dark-adaptation of the human rod system. *Vision Research, 24,* 841–849.

Owsley, C., Jackson, G. R., White, M., Feist, R., & Edwards, D. (2001). Delays in rod-mediated dark adaptation in early age-related maculopathy. *Ophthalmology, 108,* 1196–1202.

Pianta, M. J., & Kalloniatis, M. (2000). Characterisation of dark adaptation in human cone pathways: An application of the equivalent background hypothesis. *The Journal of Physiology, 528,* 591–608.

Pugh, E. N., Jr. (1975). Rushton's paradox: Rod dark adaptation after flash photolysis. *The Journal of Physiology, 248,* 413–431.

Rodieck, R. W. (1998). *First steps in seeing*. Sunderland, MA: Sinauer.

Roman, A. J., Schwartz, S. B., Aleman, T. S., Cideciyan, A. V., Chico, J. D., Windsor, E. A. M., et al. (2005). Quantifying rod photoreceptor-mediated vision in retinal degenerations: Dark-adapted thresholds as outcome measures. *Experimental Eye Research, 80,* 259–272.

Rushton, W. A. H. (1965). The Ferrier lecture, 1962: Visual adaptation. *Proceedings of the Royal Society B, 162,* 20–46.

Sakitt, B. (1972). Counting every quantum. *The Journal of Physiology, 223,* 131–150.

Sharpe, L. T., & Nordby, K. (1990). The photoreceptors in the achromat. In R. F. Hess, K. Nordby, & L. T. Sharpe (Eds.), *Night vision: Basic, clinical and applied aspects* (pp. 335–389). Cambridge, UK: CUP.

Stiles, W. S., & Crawford, B. H. (1932). Equivalent adaptational levels in localized retinal areas. In *Report of a joint discussion on vision* (pp. 194–121). Cambridge, UK: Physical Society of London, CUP. (Reprinted from *Mechanisms of colour vision* by W. S. Stiles, 1978, London: Academic Press)

Thomas, M. M., & Lamb, T. D. (1999). Light adaptation and dark adaptation of human rod photoreceptors measured from the *a*-wave of the electroretinogram. *The Journal of Physiology, 518,* 479–496.